Neuroradiology (1998) 40: 727–733

L. D'Incerti
L. Farina
I. Moroni
G. Uziel
M. Savoiardo

L-2-Hydroxyglutaric aciduria: MRI in seven cases

Received: 5 January 1998
Accepted: 22 April 1998

L. D'Incerti · L. Farina · M. Savoiardo
Department of Neuroradiology,
Istituto Nazionale Neurologico "C. Besta",
Via Celoria 11, I-20133 Milan, Italy
Tel.: +39-02-2394449
Fax: +39-02-7063 8217

I. Moroni · G. Uziel
Department of Child Neurology,
Istituto Nazionale Neurologico "C. Besta",
Milan, Italy

Abstract The MRI findings in 7 patients with L-2-Hydroxyglutaric aciduria (L-2-OHG aciduria) are described and compared with previous neuroradiological reports and the only three published pathological cases. Signal abnormalities involved peripheral subcortical white matter, basal ganglia and dentate nuclei. Cerebellar atrophy was present. Although similar appearances may be seen in other metabolic disorders, the distribution of signal abnormalities in L-2-OHG aciduria is highly characteristic and may suggest the correct diagnosis.

Key words L-2-Hydroxyglutaric aciduria · Brain, magnetic resonance imaging

Introduction

L-2-Hydroxyglutaric (L-2-OHG) aciduria is a recently described rare metabolic disorder in the group of organic acidurias (OA) affecting exclusively the central nervous system [1]. The disease is inherited as an autosomic recessive trait and is expressed as a progressive encephalopathy.

Clinically, it is characterised by mild psychomotor delay in the first years of life; later, intellectual impairment becomes evident and frequently evolves into a true dementia. Ataxia, pyramidal and extrapyramidal signs are also present. Seizures and macrocephaly have been reported in most of the patients. Differently from other OA, episodes of acute metabolic decompensation do not occur and brain damage is not related to acidosis or other metabolic imbalance [1].

Biochemically, L-2-OHG aciduria is characterised by increased concentration of L-2-OHG acid in urine, blood and cerebrospinal fluid. The metabolic defect is still undefined [2–7]. The diagnosis is obtained by detection of increased level of L-2-OHG acid in urine by means of gas chromatography-mass spectrometry [3]. The absolute configuration of the 2-OHG acid should also be obtained: in normal subjects' urine, 2-OHG acid is equally present in D and L configurations. Two different clinical entities, marked respectively by an increase in the L or D isoform, have been identified. D-2-OHG aciduria is a severe neurological syndrome with neonatal onset, whereas L-2-OHG aciduria is usually associated with a slowly progressive encephalopathy [1, 8]. Most reports on L-2-OHG aciduria have focussed on the clinical and biochemical features; the neuroradiological findings are incompletely or less frequently reported [1–14]. A detailed description of the neuroradiological features was given by Van der Knaap and Valk [15, 16].

Patients and methods

We examined seven patients between 5 and 21 years (Table 1). Diagnosis was obtained by gas chromatography-mass spectrometry of urine in all cases [3, 5].

Patients 3 and 4 were brothers. Cerebellar ataxia was evident in all patients. Except for mild motor delay, already present at 8 months in patient 5, all patients did well for the first years of life.

Table 1 Clinical data (– absent, + mild or rare, ++ moderate or moderately frequent, +++ severe or very frequent

Case	Sex	Age (years)	Onset (years)	Seizures	Pyramidal features	Extrapyramidal features	Cerebellar signs	Macrocephaly	Dementia
1	F	20	2	Febrile	+	+	+	+	+
2	M	7	4	+	+	+/–	+	+	+/–
3	M	9	4	–	+	+/–	+	+	+
4	M	5	3	–	+	–	+	+	+/–
5	M	20	8 months	+++	++	+	+	–	+
6	F	15	3	Febrile	++	+/–	++	–	++
7	F	21	4	++	+++	+	+++	–	+++

Table 2 Radiological findings (+ mild, ++ moderate, +++ marked, ++++ very severe; *A* asymmetrical signal intensity refers to T2-weighted images)

Case	Sulcal enlargement	Ventricular enlargement	Cerebellar atrophy	White matter high signal	Globus pallidus high signal	Putamen high signal	Caudate nuclei high signal	Thalamus low signal	Dentate nuclei high signal
1	+	++	+	+++	+	+	–	++	+
2	–	+	–	++	+	+	–	++	++
3	–	+	+	++	++	+	–	++	++
4	+	+	+	+++	++	+	+	++	++
5	–	+	+	++++	+A	–	–	++	+
6	–	+	+	++++	+	–	–	++	++
7	–	++	++	++++	+A	–	–	++	–

Patients 2 and 5 developed seizures as the first symptom. Mental impairment and pyramidal signs also appeared in all patients; in the older ones (patients 1, 5 and 7) the disease worsened into a severe dementia associated with progressive paraparesis. Patient 7 died at the age of 21 years. Patients 2, 3 and 4 were only mildly impaired. Macrocephaly was observed in patients 1–4.

All patients underwent at least one MRI examination; three patients had two and one had four MRI studies, giving a total of 13 MRI examinations. A 0.5 T unit was employed in eight examinations; the others were obtained with a 1.5 T machine. All examinations included sagittal T1-weighted images obtained with spin-echo (SE) or gradient-echo (fast-field echo, FFE) techniques. Axial and coronal intermediate and T2-weighted images (SE 1900–2000/30–50 and 90–120 ms) were also obtained in all cases. In six cases axial and coronal T1-weighted images (SE 300–600/15–20 ms) were obtained. In two cases studied at 1.5 T, coronal FFE (24/30 ms, 30°) and axial FLAIR (8000/150/1900 ms) slices were obtained. The MRI studies were reviewed by three different neuroradiologists experienced in neurometabolic disorders. The following were considered: location, morphology and extent of white matter (WM) and basal ganglia abnormalities; size and shape of the ventricles and peripheral subarachnoid space; cerebellar abnormalities.

The extent of WM and basal ganglia abnormalities and of atrophic changes was subjectively rated as mild (+), moderate (++), marked (+++) and very severe (++++). Particular attention was also given to the extent of the WM abnormalities on T1-weighted images.

The only CT study performed (in case 2) was also reviewed.

Results

Neuroradiological data are summarised in Table 2. MRI demonstrated fairly symmetrical signal abnormalities involving the WM of the cerebral hemispheres and prevailing in the subcortical areas. Bilateral abnormalities in the basal ganglia were present in all patients. In six cases, bilateral involvement of the dentate nuclei was seen. Enlargement of the cerebellar sulci and of the fourth ventricle was present in six cases: it was mild in five and more marked only in case 7. WM abnormalities were demonstrated on both T1- and T2-weighted images.

On the basis of the extent of the WM lesions, the cases were divided into two groups: group 1 had multifocal, and group 2 diffuse, confluent lesions.

Group 1 (patients 1–4)

Scattered WM lesions, high-signal on T2-weighted images, were in the cores of the cerebral convolutions with little or no extension to the deep lobar WM and even less involvement of the periventricular WM (Fig. 1). On T1-weighted images only the subcortical involvement was recognisable; the cortical ribbon was normal with sharp separation from the subcortical low signal intensity, which faded in centripetal direction.

In three of these cases studied at 1.5 T enlargement of the perivascular spaces in the frontal and parietal gyri and the centra semiovalia was observed (Fig. 2), more evident on T1-weighted images. In the most cranial axial FLAIR images, the perivascular spaces stood out as tiny dots of low signal within the high signal of the abnormal surrounding WM (Fig. 2).

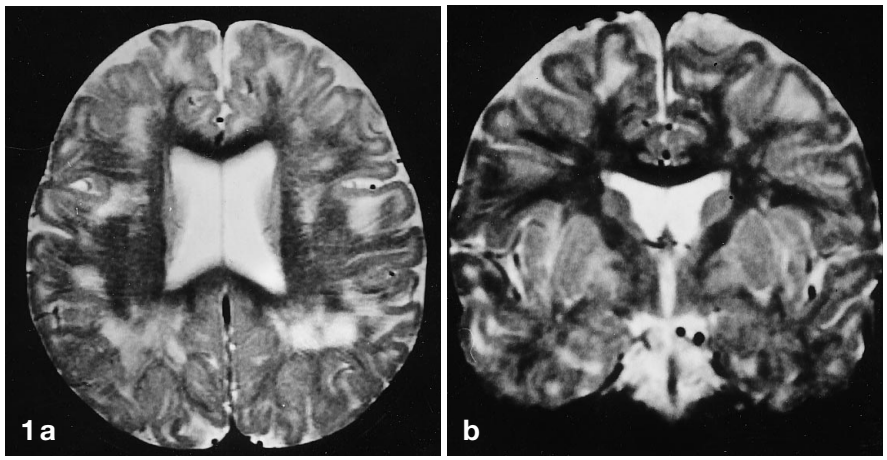

Fig. 1 Axial (**a** case 4) and coronal (**b** case 3) T2-weighted images show scattered areas of high signal mainly involving subcortical white matter

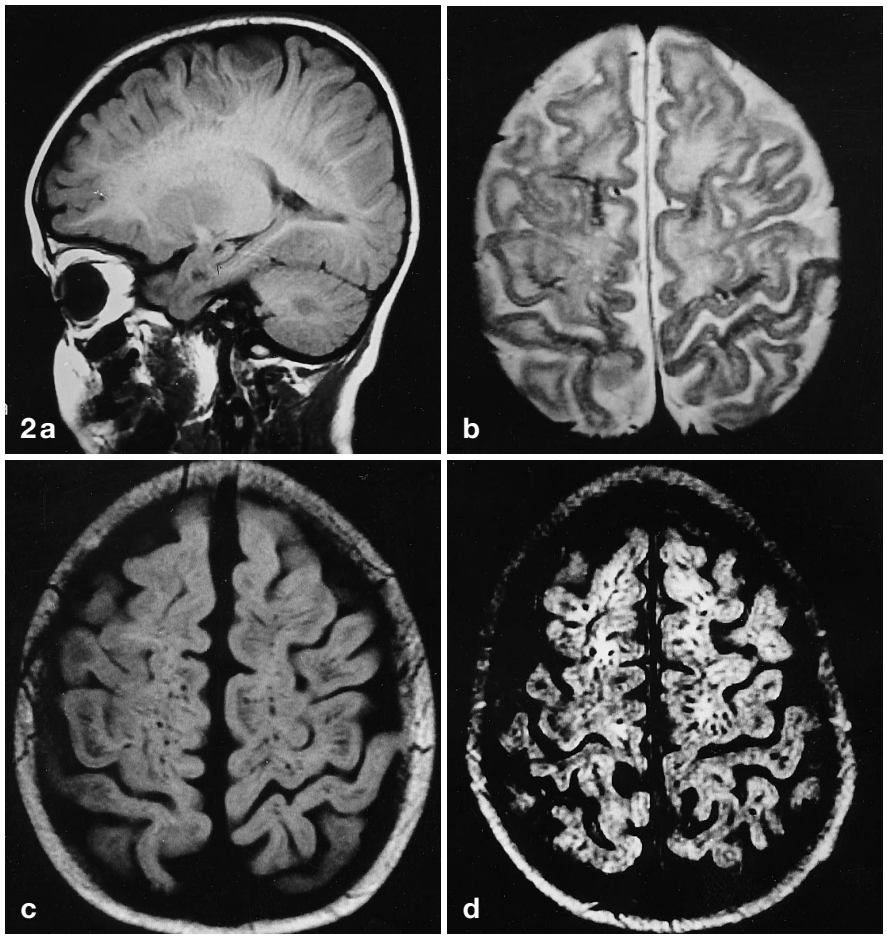

Fig. 2a–d Case 3. **a** Sagittal T1-weighted image shows enlargement of perivascular spaces. **b** In a T2-weighted image these are isointense with the abnormal white matter. They are recognisable as dots of low signal on an axial T1-weighted image (**c**) and more obvious on a FLAIR image (**d**), in which they stand out against the high signal of the abnormal white matter

WM abnormalities were more marked in the younger of the two brothers (case 4).

In all of this group, symmetrical high signal in the globus pallidus (Fig. 3) and dentate nuclei (Fig. 4) was present on T2-weighted images. On T1-weighted images, the dentate nuclei were hypointense, while the abnormalities of the globus pallidus were not recognisable.

In all cases, slightly high signal was seen on T2 weighting in the putamina and, in case 4, in the head of the caudate nuclei (Fig. 3).

In this group, mild enlargement of the lateral ventricles and, in cases 1 and 4, of the cerebral sulci was seen. In case 3, widening of the anterior part of the Sylvian fissure was evident. In cases 1, 3 and 4, mild en-

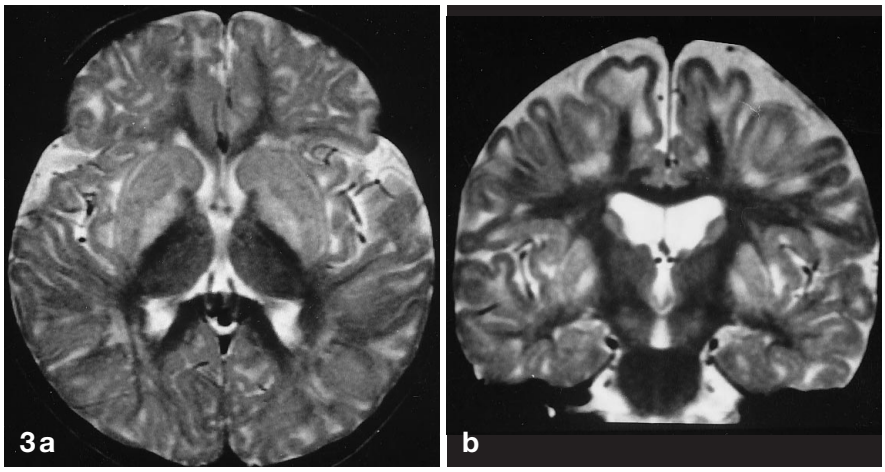

Fig. 3a, b Case 4. **a** Axial and **b** coronal T2-weighted images show bilateral, symmetrical high signal in the globus pallidus. In **b** slightly high signal is also seen in the putamina and caudate nuclei. White matter abnormalities also involve the external and extreme capsules. Axial section also demonstrates *low* signal in the thalamus

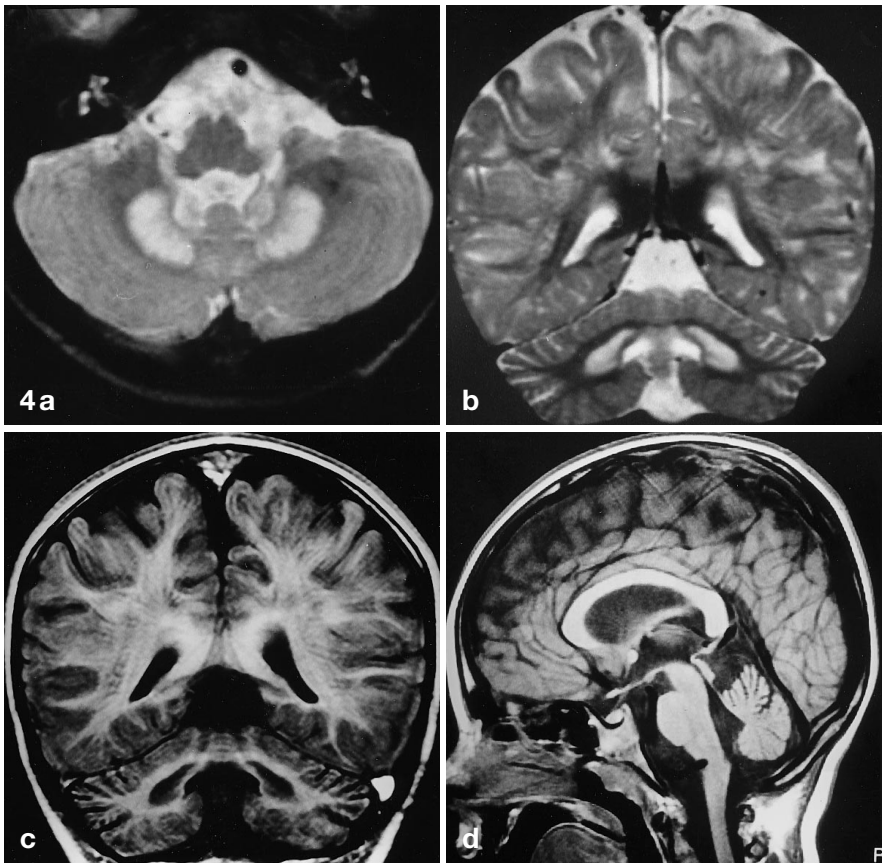

Fig. 4a–d Case 4. **a** Axial and **b** coronal T2-weighted images show bilateral, symmetrical high signal in the dentate nuclei, extending to the surrounding white matter. **c** Coronal T1-weighted image demonstrates low signal in the dentate nuclei and enlargement of the fourth ventricle. **d** Sagittal T1-weighted image confirms the enlargement of the fourth ventricle and shows mild enlargement of the cerebellar sulci. Indentation of the anterior aspect of the medulla oblongata is due to an elongated left vertebral artery

largement of the fourth ventricle and of the cerebellar sulci was seen. In patient 1, who underwent 4 MRI studies in 3 years, increasing enlargement of the frontal horns associated with shrinkage of the frontal WM was observed. Patients 3 and 4 each had two MRI examinations in 2 years: no progression of the radiological picture was observed.

In the only CT study performed (in case 2), faint low density involved the subcortical cerebral WM and the dentate nuclei. The distribution of the abnormalities was the same as on MRI.

Group 2 (patients 5–7).

In this group the areas of high signal on T2-weighted images were diffuse and confluent (Fig. 5). Involvement of the deep WM, although incomplete, was more

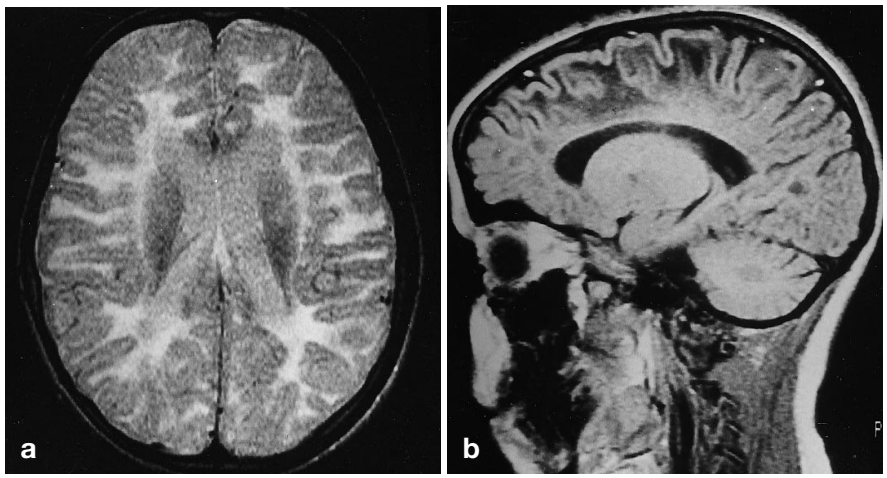

Fig. 5 a, b Case 6. **a** Axial T2-weighted image shows diffuse high signal in white matter. **b** Sagittal T1-weighted image demonstrates the prevalence of the white matter abnormalities in the subcortical areas

marked than in group 1. WM abnormalities on T1-weighted images were limited to the subcortical regions, which appeared of low signal (Fig. 5). In case 7, mild swelling of the cerebral convolutions was present.

In all of this group, mildly increased signal was present on T2 weighting in the globus pallidus, asymmetrical in cases 5 and 7. No signal abnormalities were observed in the putamina or in the caudate nuclei. In cases 5 and 6, high signal on T2- and low signal on T1-weighted images was present in the dentate nuclei, with mild extension to the surrounding WM.

In all cases, slight enlargement of the lateral ventricles was present, asymmetrical in case 7. In this case, 2-year follow-up revealed increasing enlargement of the lateral ventricles. This patient also had a moderate enlargement of the fourth ventricle and the cerebellar sulci.

MRI findings common to groups 1 and 2

In all cases the WM abnormalities involved the external and the extreme capsules. Similarly in all cases, pallidal high signal and thalamic low signal were present on T2-weighted images (Fig. 3). The corpus callosum and brain stem were always spared.

Discussion

Correlation between MRI findings and pathology in our series of L-2-OHG aciduria could not be obtained: in the only patient who died (case 7), permission for post-mortem examination was not granted. A comparison between MRI findings and neuropathology can be made with three cases reported in the literature with different clinical and pathological features [6, 17, 18].

The first report describes the results of postmortem examination of a 17-year-old woman who died of a brain tumour; L-2-OHG aciduria was diagnosed at age 15 years [6]. The second includes the pathological findings in a 30-year-old man [17], the third, those of a neonate who died at 28 days [18].

In our series, the main MRI abnormalities were in the WM, cerebellum and basal ganglia. Their combined occurrence is highly suggestive of L-2-OHG aciduria [15, 16], but, for a thorough discussion, each of these aspects and their combination will be analysed and compared with similar MRI findings occurring in other metabolic disorders and with the three pathological reports mentioned above on L-2-OHG aciduria.

The most striking MRI abnormalities consisted of scattered or diffuse subcortical WM abnormalities fading centripetally. The pathological cases described by Wilcken et al. [6] and Larnaut et al. [17] showed spongiosis and cystic cavitation in subcortical WM. This distribution, however, is not only limited to L-2-OHG aciduria: it may be observed on MRI and in pathological cases in Canavan's disease, Kearns-Sayre syndrome and OA, that also have spongy degeneration [15, 16, 19]. Spongy degeneration of different origin, therefore, may behave in the same way, affecting first the subcortical WM with subsequent centripetal extension [15, 16, 19, 20]. The greater vulnerability of the subcortical WM might depend on its later myelination [15]. Otherwise, any pathological change involving the younger, newly formed WM results in a spongy degeneration [19].

In L-2-OHG aciduria, the subcortical abnormalities are perhaps more severe than in Kearns-Sayre syndrome and other OA since they are clearly visible on T1 weighting. We wish to stress the role of T1-weighted images in cases of L-2-OHG aciduria in which T2-weighted images demonstrate diffuse high signal in the cerebral WM; although the immediately periventricular WM and the corpus callosum were spared, T2-weighted images of these cases suggested extensive leukodystrophic disease (Fig. 5). Due to their lower sensitivity to

WM abnormalities, the T1-weighted images made it possible to identify the regions in which the pathological changes were more marked, i.e., the subcortical areas, where the disease probably started (Fig. 5), thus adding a diagnostic clue.

Progression of the atrophy of the WM and clinical worsening were observed in cases 1 and 7, two of the four patients in whom follow-up studies were available. However, the MRI of patient 2, who was very mildly affected and referred only for seizures, showed extensive involvement of WM. This observation suggests that MRI abnormalities may be present in the very early stages of the disease and perhaps even in presymptomatic subjects.

Apart from case 1, the three patients in whom WM abnormalities were diffuse and confluent (group 2) were the oldest and had a more severe clinical picture. This suggests a correlation between the severity of the MRI picture and the clinical findings. Nevertheless, the elder of the two brothers (cases 3 and 4) had more severe neurological disturbances, whereas the MRI abnormalities were more extensive in the younger one. In these two cases, no clinical or radiological changes were observed over a 2-year follow-up.

Unlike the cases in the literature [2–7, 9, 13, 15, 16, 18], cerebellar atrophy was not constant in our cases. Cerebellar disturbances, which were present in all our patients, could be related both to cerebellar atrophy and to selective involvement of the dentate nuclei. In patient 7, however, no abnormalities of the dentate nuclei were observed, while cerebellar atrophy was more marked than in the other cases.

In six of seven cases, signal abnormalities were seen in the dentate nuclei on both T2- and T1-weighted images (Fig. 4). As with the subcortical WM abnormalities, the low signal on T1-weighting of the dentate nuclei may suggest severe, longstanding involvement since the early stages of the disease. This hypothesis is supported by the pathological findings in a neonate, consisting of severe cell loss and gliosis in the dentate nuclei and astrocytosis of the cerebellar white matter; cell loss and gliosis also involved pontine and inferior olivary nuclei [18]. Marked cell loss and severe spongiosis of the dentate nuclei were also reported by Larnaut et al. [17]. Therefore, the abnormalities in the dentate nuclei observed on MRI in our patients also correspond to the pathological findings.

Signal abnormalities in the dentate nuclei and in the surrounding cerebellar white matter are reported in some cases of Leigh's disease with cytochrome-c-oxidase deficiency; signal abnormalities are also often present in the dorsal brain stem and subthalamic nuclei [21]. In our cases of L-2-OHG aciduria, no associated abnormalities were seen in the brain stem.

Cell loss and spongiosis have been described in the globus pallidus by Larnaut et al. [17]. We observed pallidal high signal on T2 weighting, less marked than in the dentate nuclei, in all our cases of L-2-OHG aciduria (Fig. 3). Pallidal abnormalities were not recognisable on T1-weighted images, probably because spongiosis in these nuclei is less severe than in the peripheral white matter and dentate nuclei, as the pathological report by Larnaut et al. [17] also suggests.

Among the OA, pallidal abnormalities are frequently observed as the only change in methylmalonic acidaemia (MMA) [16, 22], but they are very marked and not associated with the other abnormalities observed in L-2-OHG aciduria. Abnormal signal intensity in the globus pallidus, associated with WM abnormalities, can also be seen in other OA [11].

In all four patients of group 1, slightly increased signal involved the putamina and in case 4 also the caudate nuclei (Fig. 3). A similar pattern can occur in other metabolic disorders, such as mitochondrial encephalopathies, particularly Leigh's disease, but with much more marked high signal [15, 19].

In all our patients, striking low signal was observed in the thalamus on T2-weighted images (Fig. 3). A similar finding has been reported in many degenerative disorders. The low signal may be related to deposition of iron or other paramagnetic substances [23].

Macrocephaly was present only in group 1; in the literature this feature is said to be very frequent [14]. A possible explanation for this discrepancy is that macrocephaly is related to the early onset of the disease and age of observation. Our patients with macrocephaly were the younger ones (except for patient 1, whose age at first observation was 18 years), like most previously reported cases. In all these cases, macrocephaly probably occurred because the disease started before the closure of the cranial sutures and was probably associated with swelling of the convolutions. Disappearance of swelling followed by atrophy of the WM probably accounts for the absence of macrocephaly in older patients.

In case 3, we observed enlargement of the Sylvian fissures: this findings is more frequently described, and is perhaps characteristic, in glutaric aciduria type 1 [11, 15, 24]. It is supposed to be secondary to abnormal development of the anterior temporal regions associated with an anomalous splitting of the arachnoid membrane and has been rarely observed in different forms of neurological OA such as MMA and glutaric aciduria type 2 [11].

The MRI picture in our patients thus shows a good correlation with the very few pathological data and are very similar to those described by Van der Knaap and Valk [15, 16]. Separation between mildly and severely affected patients corresponds to a different distribution and severity of WM and putaminal involvement. MRI abnormalities in the peripheral subcortical white matter and dentate nuclei are almost always observed

and seem to be related to pathological changes which probably occurred at the beginning of the disease. Involvement of the basal ganglia, particularly the globus pallidus, is constant but less severe. Cerebellar atrophy, almost aways reported in other series, was obvious only in one of our patients. The absence of such abnormality, therefore, does not exclude the diagnosis.

When we consider the combination of the various abnormalities described in the WM, dentate nuclei, globus pallidus and thalamus we have a "Gestalt" with little or no differential diagnosis; only a few other OA or mitochondrial disorders should be considered. Their observation, therefore, should prompt gas chromatography-mass spectrometry which can confirm the diagnosis.

References

1. Hoffmann GF, Gibson KM, Trefz FK, et al (1994) Neurological manifestations of organic acid disorders. Eur J Pediatr 153 [Suppl 1] 94–100
2. Barth PG, Hoffmann GF, Jaeken J, et al (1992) L-2-Hydroxyglutaric acidemia: a novel inherited neurometabolic disease. Ann Neurol 32: 66–71
3. Barth PG, Hoffmann GF, Wanders RJ (1993) L-2-Hydroxyglutaric acidemia: clinical and biochemical findings in 12 patients and preliminary report on L-2-hydroxyacid dehydrogenase. J Inher Metab Dis 16: 753–761
4. Divry P, Jakobs C, Vianey-Saban C, Gibson KM, et al (1993) L-2-Hydroxyglutaric aciduria: two further cases. J Inher Metab Dis 16: 505–507
5. Duran M, Kamerling JP, Bakker HD, et al (1980) L-2-Hydroxyglutaric aciduria: an inborn error of metabolism? J Inher Metab Dis 3: 109–112
6. Wilken B, Pitt J, Heath D, et al (1993) L-2-Hydroxyglutaric aciduria: three Australian cases. J Inher Metab Dis 16: 501–504
7. Gibson KM, Craigen W, Herman GE, et al (1993) D-2-Hydroxyglutaric aciduria in a newborn with neurological abnormalities: a new neurometabolic disorder? J Inher Metab Dis 16: 497–500
8. Gibson KM, Brink HJ, Schor DS, et al (1993) Stable-isotope dilution analysis of D- and L-2-Hydroxyglutaric acid: application to the detection and prenatal diagnosis of D- and L-2-Hydroxyglutaric acidemias. Pediatr Res 34: 277–280
9. Barbot C, Fineza I, Diogo L, et al (1997) L-2-Hydroxyglutaric aciduria: clinical, biochemical and magnetic resonance imaging in six Portuguese pediatric patients. Brain Dev 19: 268–273
10. Hoffmann GF, Jakobs C, Holmes B, et al (1995) Organic acids in cerebrospinal fluid and plasma of patients with L-2-Hydroxyglutaric aciduria. J Inher Metab Dis 18: 189–193
11. Brismar J, Ozand PT (1994) CT and MR of the brain in the diagnosis of organic acidemias: experiences from 107 patients. Brain Dev 16 [Suppl]: 104–124
12. Jaecken J, Willekens H, Corbeel L (1988) Leukodystrophy associated with hypoerlysinirachia and 2-hydroxyglutaric aciduria. Pediatr Res 24: 266
13. Hanenfeld F, Kruse B, Bruhn H (1994) In vivo proton resonance spectroscopy of the brain in a patient with L-2-Hydroxyglutaric acidemia. Pediatr Res 35: 614–616
14. Kaabachi N, Larnaut A, Rabier D, et al (1993) Familial encephalopathy and L-2-Hydroxyglutaric aciduria. J Inher Metab Dis 16: 893
15. Van der Knaap MS, Valk J, Barth PG, et al (1995) Leukoencephalopathy with swelling in children and adolescents: MRI patterns and differential diagnosis. Neuroradiology 37: 679–686
16. Van der Knaap MS, Valk J (1995) Magnetic resonance of myelin, myelination, and myelin disorders. 2nd edn. Springer, Berlin Heidelberg New York, pp 22–30, 201–204, 220–223
17. Larnaut A, Hentati F, Belal S, et al (1994) Clinical and pathological study of three Tunisian siblings with L-2-Hydroxyglutaric aciduria. Acta Neuropathol 88: 367–370
18. Chen E, Nyhan W, Jakobs C, et al (1996) L-2-Hydroxygluatric aciduria: neuropathologic correlations and first report of severe neurodegenerative disease and neonatal death. J Inher Metab Dis 19: 335–343
19. Barkovich AJ, Good WV, Koch TK, et al (1993) Mitochondrial disorders: analysis of their clinical and imaging characteristics. AJNR 14: 1119–1137
20. Friede RL (1989) Developmental neuropathology, 2nd edn. Springer, Berlin Heidelberg New York, pp 510–523
21. Savoiardo M, Uziel G, Strada L, et al (1991) MRI findings in Leigh's disease with cytochrome-c-oxidase deficiency. Neuroradiology 33 [Suppl]: 507–508
22. Brismar J, Ozand P (1994) CT and MR of the brain in disorders of the propionate and methylmalonate metabolism. AJNR 15: 1459–1473
23. Atlas SW (1996) Magnetic resonance imaging of the brain and spine, 2nd edn. Lippincott-Raven, Philadelphia, pp 814–816
24. Naidu S, Moser HW (1991) Value of neuroimaging in metabolic diseases affecting the CNS. AJNR 12: 413–416